
Electroweak Measurements of Multiboson Production with the ATLAS Experiment

Stefanie Götz on behalf of the ATLAS Collaboration

Ludwig-Maximilians-Universität München

ICNFP 2024

2 Sep 2024

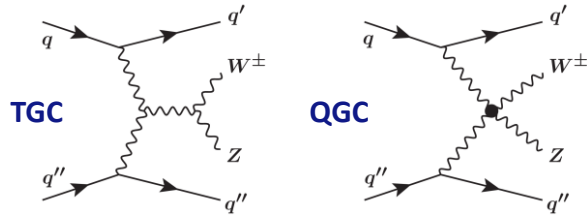


Bundesministerium
für Bildung
und Forschung



Multiboson studies probe the SM EW symmetry breaking mechanism

- Study of vector boson **self-couplings**
 - ⇒ Vector boson self-interactions determined by the gauge symmetry of the EW theory
 - ⇒ **VBS** of particular interest due to its sensitivity to triple and quartic gauge couplings

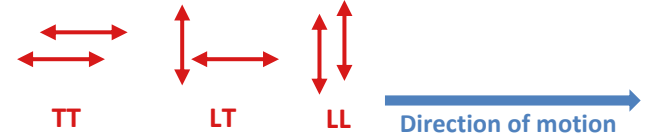


- ⇒ Search for anomalous gauge couplings in context of an **EFT interpretation**

$$\mathcal{L}_{\text{eff}} = \mathcal{L}_{\text{SM}} + \sum_i \frac{f_i^{(6)}}{\Lambda_i^2} O_i^{(6)} + \sum_i \frac{f_i^{(8)}}{\Lambda_i^4} O_i^{(8)} + \dots$$

EFT
SM
aTGC
aQGC

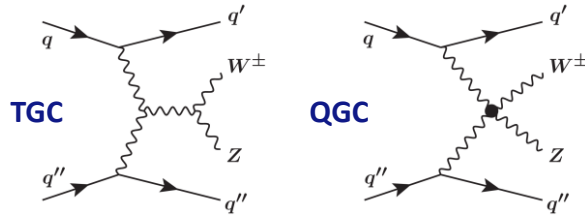
- Study of vector boson **polarisation states**
 - ⇒ Vector bosons obtain through the EW symmetry breaking mechanism longitudinally polarised states



- ⇒ Deviations of the cross-section of the longitudinal polarisation state indicates physics beyond the SM

Multiboson studies probe the SM EW symmetry breaking mechanism

- Study of vector boson **self-couplings**
 - ⇒ Vector boson self-interactions determined by the gauge symmetry of the EW theory
 - ⇒ **VBS** of particular interest due to its sensitivity to triple and quartic gauge couplings

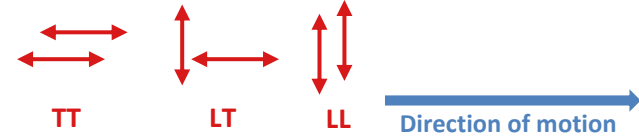


- ⇒ Search for anomalous gauge couplings in context of an **EFT interpretation**

$$\mathcal{L}_{\text{eff}} = \mathcal{L}_{\text{SM}} + \sum_i \frac{f_i^{(6)}}{\Lambda_i^2} O_i^{(6)} + \sum_i \frac{f_i^{(8)}}{\Lambda_i^4} O_i^{(8)} + \dots$$

EFT
SM
aTGC
aQGC

- Study of vector boson **polarisation states**
 - ⇒ Vector bosons obtain through the EW symmetry breaking mechanism longitudinally polarised states

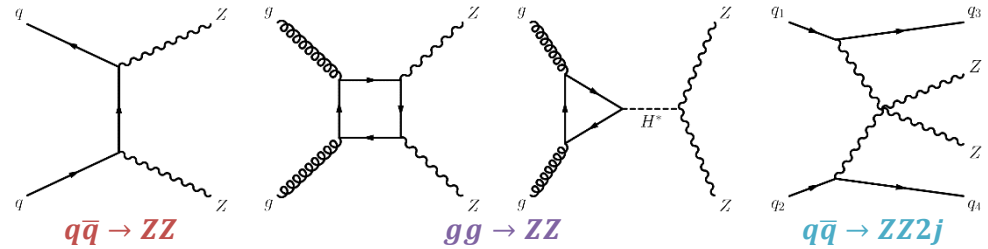


- ⇒ Deviations of the cross-section of the longitudinal polarisation state indicates physics beyond the SM

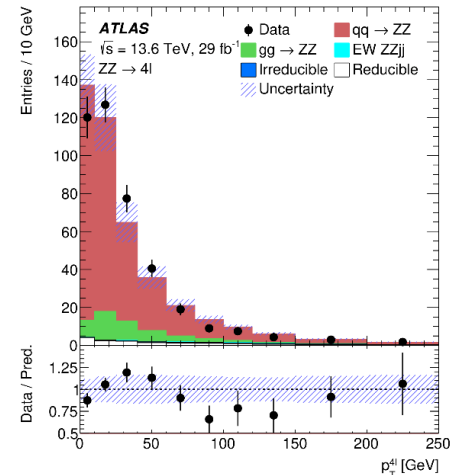
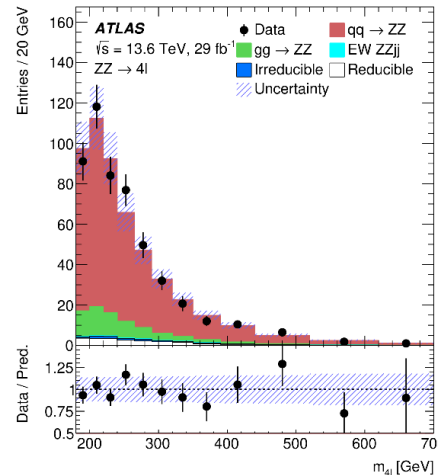
ATLAS analyses presented in this talk

- New energy:** ZZ at 13.6 TeV
- Polarisation:** ZZ polarisation & CP WZ polarisation at high p_T
- VBS:** $W^\pm Zjj$ $W^\pm W^\pm jj$ $W\gamma jj$

- **First Run-3 ZZ cross-section measurement!**
- Rarest diboson process but attractive due to high signal-to-background ratio in fully-leptonic channels
- Key channel for aTGCs searches & studying off-shell Higgs boson production
- **Signal:** 2 SFOC lepton pairs (e, μ) with on-shell Z requirements
- $q\bar{q} \rightarrow ZZ$ dominant process
- Irreducible backgrounds from $t\bar{t}Z$ & triboson
- Non-prompt lepton background
- Comparison of results to state-of-art MC simulation and fixed-order calculations (NNLO QCD & NL EW)



Good data/MC agreement!

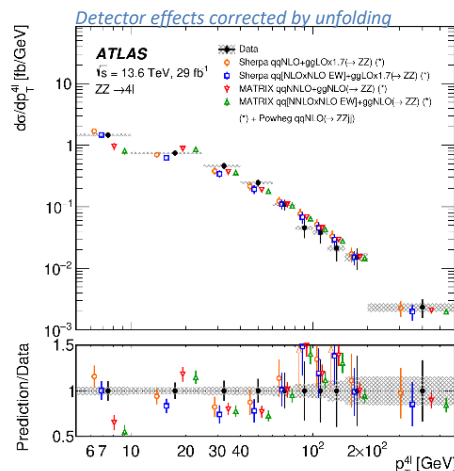
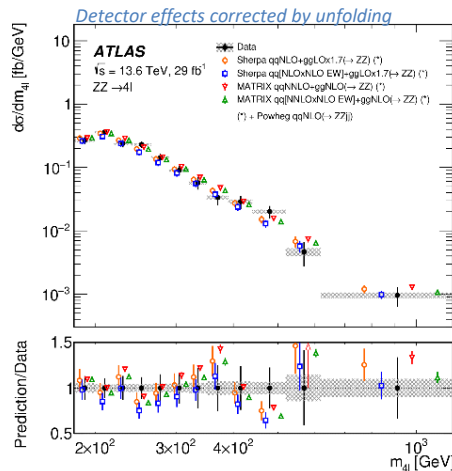


Cross-section measurements:

- Inclusive measurement & extrapolation to a total phase space with $66 < m_Z < 116\text{GeV}$

| | Measurement | MC prediction | MATRIX prediction |
|----------|--|---------------------------------|---------------------------|
| Fiducial | $36.7 \pm 1.6(\text{stat}) \pm 1.5(\text{syst}) \pm 0.8(\text{lumi}) \text{ fb}$ | $36.8^{+4.3}_{-3.5} \text{ fb}$ | $36.5 \pm 0.7 \text{ fb}$ |
| Total | $16.8 \pm 0.7(\text{stat}) \pm 0.7(\text{syst}) \pm 0.4(\text{lumi}) \text{ pb}$ | $17.0^{+1.9}_{-1.4} \text{ pb}$ | $16.7 \pm 0.5 \text{ pb}$ |

- Differential measurements



ZZ at 13.6 TeV in a historical context:

- Extension of diboson studies to a **new centre-of-mass energy**

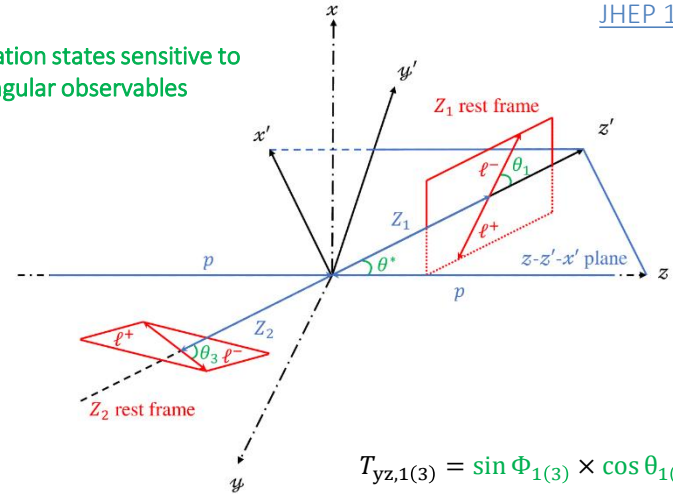


All results well described by SM predictions!

ZZ polarisation & CP

- **Signal:** $q\bar{q} \rightarrow ZZ, gg \rightarrow ZZ, qq \rightarrow ZZjj$
- 2 SFOC e or μ pairs, on-shell with $|m_{H1} - m_Z| < 10$ GeV
- Prompt lepton background from $t\bar{t}Z$ & triboson
- Non-prompt lepton background
- 3 helicity states: $Z_L Z_L, Z_L Z_T, Z_T Z_T$
- $Z_L Z_L$ signal extraction by profile likelihood fit on BDT distribution
- Additional reweighting of MC templates to account for NLO/LO corrections of ZZ polarisation states

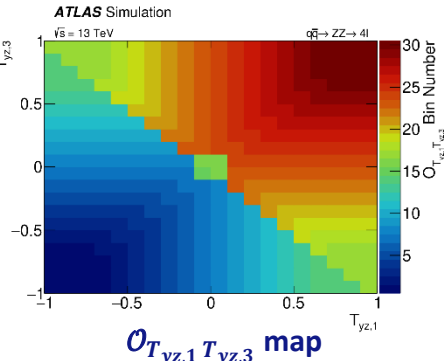
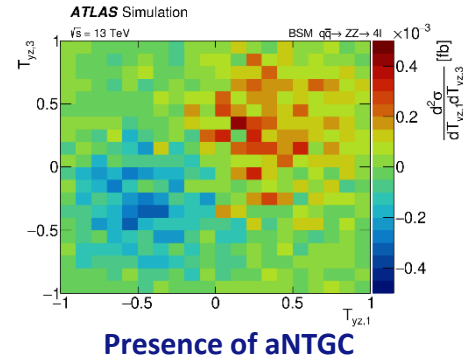
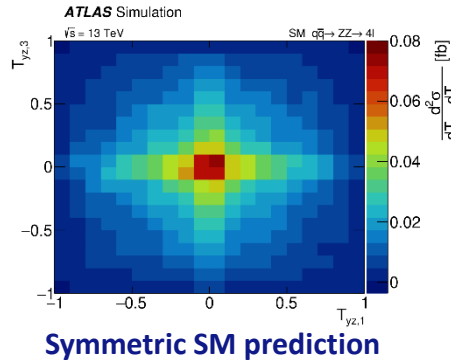
Polarisation states sensitive to angular observables



$$T_{yz,1(3)} = \sin \Phi_{1(3)} \times \cos \theta_{1(3)}$$

- **aNTGC** cross-section: $\sigma^i = \sigma_{SM}^i + c\sigma_{interference}^i + c^2\sigma_{quadratic}^i$

- Construction of an observable $\mathcal{O}_{T_{yz,1} T_{yz,3}}$ to improve sensitivity to CP-odd aNTGC



Polarisation measurements:

$$\sigma_{Z_L Z_L}^{\text{obs}} = 2.45 \pm \underset{\text{stat}}{0.56} \pm \underset{\text{syst}}{0.21} \text{ fb with } 4.3\sigma \text{ significance}$$

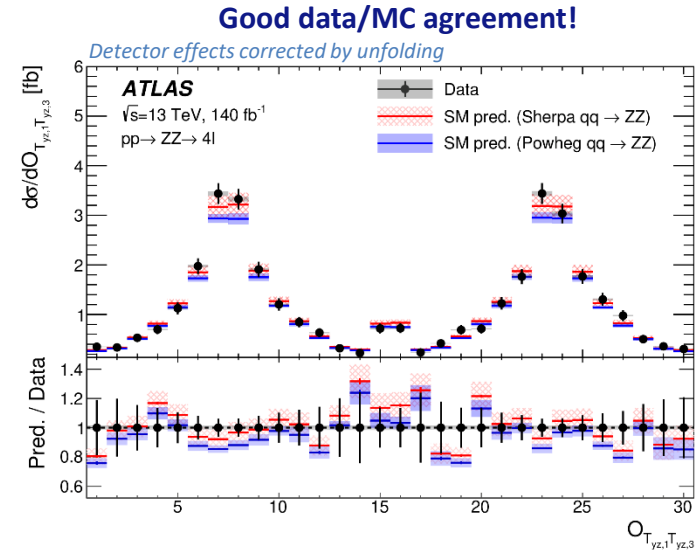
- $Z_L Z_L$ -polarisation cross-section consistent with SM prediction
- Measurement limited by data statistic & polarisation modelling

Study of the CP property :

- Inclusive ($Z_L Z_L + Z_L Z_T + Z_T Z_T$) differential cross-section measurement for $\mathcal{O}_{T_{yz,1} T_{yz,3}}$
- $\mathcal{O}_{T_{yz,1} T_{yz,3}}$ asymmetric for CP-odd aNTGC

CP-odd aNTGC:

- Constraints on ZZZ & $ZZ\gamma$ coupling parameters f_Z^4, f_γ^4 at 95% CL using the differential cross-section distribution
- First constraints using only linear interference terms
- **No significant deviations from SM**



CP-odd aNTGC

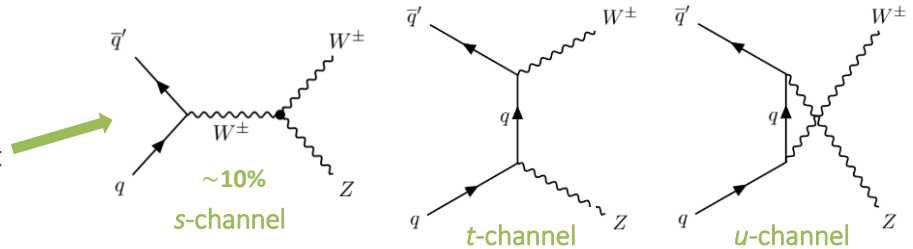
with $\sigma^i_{\text{quadratic}}$

| aNTGC parameter | Interference only | | Full | |
|-----------------|-------------------|---------------|-----------------|-----------------|
| | Expected | Observed | Expected | Observed |
| f_Z^4 | [-0.16, 0.16] | [-0.12, 0.20] | [-0.013, 0.012] | [-0.012, 0.012] |
| f_γ^4 | [-0.30, 0.30] | [-0.34, 0.28] | [-0.015, 0.015] | [-0.015, 0.015] |

WZ polarisation at high p_T

- **Signal:** $Z \rightarrow l'l'$ (SFOC) with $|m_{ll} - m_Z| < 10$ GeV
 $W \rightarrow l\nu$ with $m_T^W > 30$ GeV
 $l = e, \mu$

Measurement in **s-channel** to obtain a sufficient contribution of 00 WZ polarisation states



- Selection of 2 fiducial regions such to enhanced prevalence for the 2 longitudinally-polarised (00) bosons for the measurement of **diboson polarisation fractions** $f_{00}, f_{0T}, f_{T0}, f_{TT} \Rightarrow$ **high p_T^Z**
- Exploit **Radiation Amplitude Zero (RAZ) effect in WZ**
 - \Rightarrow Dominant helicity amplitude of the TT-polarised bosons becomes zero when the scattering angle of the W boson to the incoming antiquark \bar{q} approaches 90° in the WZ restframe
 - \Rightarrow NLO QCD corrections dilute effect

Reduced jet activity for the observation of the RAZ

Reduced TT contribution and increase of f_{00} from 5-7% to 20-30%

| | Signal regions | | |
|---|--------------------------|----------------------|----------------------|
| | Radiation Amplitude Zero | 00-enhanced region 1 | 00-enriched region 2 |
| Pass inclusive WZ event selection | ✓ | ✓ | ✓ |
| Transverse momentum of the Z boson (p_T^Z) | - | [100, 200] GeV | > 200 GeV |
| Transverse momentum of the WZ system (p_T^{WZ}) | < 20, 40, 70 GeV | < 70 GeV | |

RAZ effect in WZ:

- **First-time study in WZ**
- Evaluation of the 00+0T+T0-subtracted $|\Delta Y(l_W Z)|$ & $|\Delta Y(WZ)|$ distributions for TT events
- Evaluation of the dip depth

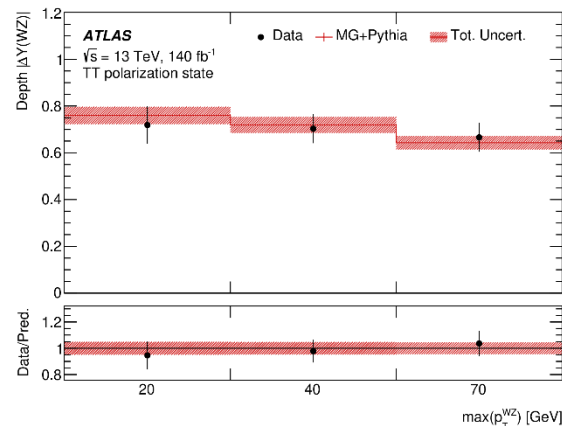
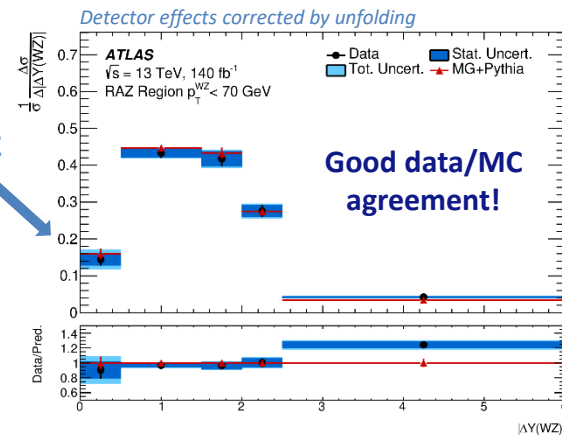
$$\mathcal{D} = 1 - 2 \frac{N_{\text{central}}^{\text{unf}}}{N_{\text{sides}}^{\text{unf}}} > 0 \text{ indicates dip}$$

Energy dependence of diboson polarisation fractions

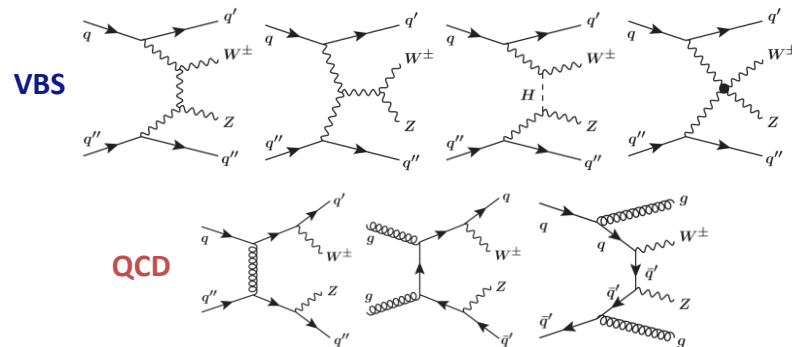
- Signal extraction from maximum-likelihood fit on BDT score distribution
- **f_{00} observation in agreement with SM prediction**

| | Measurement | |
|---------------------------------|--|--|
| | $100 < p_T^Z \leq 200 \text{ GeV}$ | $p_T^Z > 200 \text{ GeV}$ |
| f_{00} | $0.19 \pm_{0.03}^{0.03} \text{ (stat)} \pm_{0.02}^{0.02} \text{ (syst)}$ | $0.13 \pm_{0.08}^{0.09} \text{ (stat)} \pm_{0.02}^{0.02} \text{ (syst)}$ |
| f_{0T+T0} | $0.18 \pm_{0.08}^{0.07} \text{ (stat)} \pm_{0.06}^{0.05} \text{ (syst)}$ | $0.23 \pm_{0.18}^{0.17} \text{ (stat)} \pm_{0.10}^{0.06} \text{ (syst)}$ |
| f_{TT} | $0.63 \pm_{0.05}^{0.05} \text{ (stat)} \pm_{0.04}^{0.04} \text{ (syst)}$ | $0.64 \pm_{0.12}^{0.12} \text{ (stat)} \pm_{0.06}^{0.06} \text{ (syst)}$ |
| $f_{00} \text{ obs (exp) sig.}$ | $5.2 \text{ (4.3)} \sigma$ | $1.6 \text{ (2.5)} \sigma$ |

Dip indicates RAZ



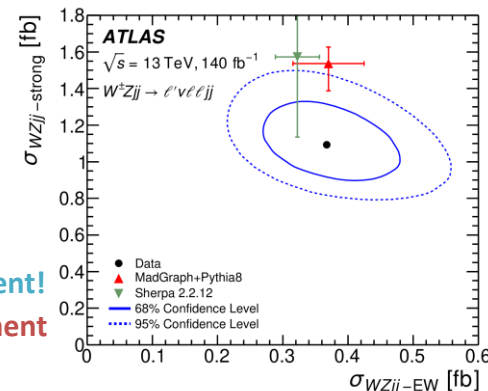
- **VBS** not independently gauge invariant, therefore study with same final-state processes required
 - ⇒ Exclusively **EW** $\sim \alpha_{EW}^6$
 - ⇒ **QCD** $\sim \alpha_S^2 \alpha_{EW}^4$
 - ⇒ EW-QCD interference $\sim \alpha_S \alpha_{EW}^5$
- **Signature:** $WZ \rightarrow l'\nu ll$ & $\geq 2j$
- SR with enhanced **VBS**: $m_{jj} > 500$ GeV, $N_{b\text{-quark}} = 0$
- Main irreducible background from ZZ & $t\bar{t}V$
- Background from misidentified leptons



EW & QCD cross-section measurements

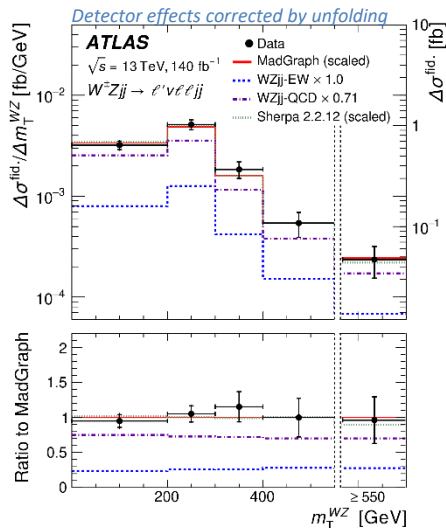
- Multivariate discriminant constructed from BDT to separate **EW** from **QCD**
- **Most precise EW $W^\pm Zjj$ cross-section measurement to date!**

Good EW agreement!
▲ 1.8σ QCD agreement



EW & QCD differential cross-section measurements

- In bins of N_{jets} , m_{jj}
- **2 σ EW agreement** in all SR sub-categories
- **QCD** mis-modelling by MADGRAPH+PYTHIA8 or SHERPA 2.2.12 for events with exactly 2 jets of $p_T > 25$ GeV or with $500 < m_{jj} < 1300$ GeV



$W^\pm Zjj$ inclusive differential cross-section measurements

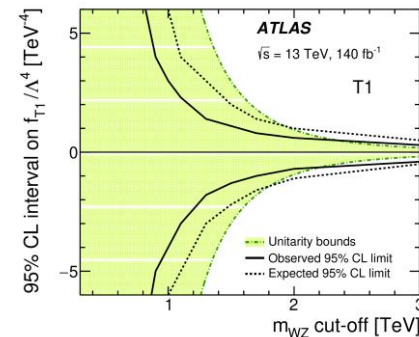
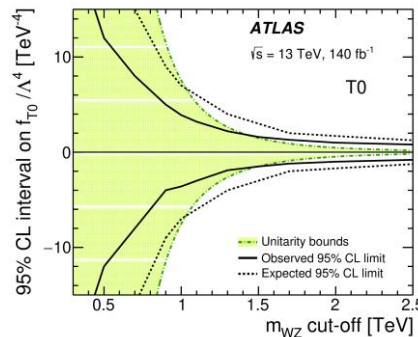
- For several kinematic observables
- Statistical uncertainties dominant

aQGC

- BDT score & m_T^{WZ} to search for aQGC
- 95% CL limits D-8 EFT operators indicating **no deviation from 0**

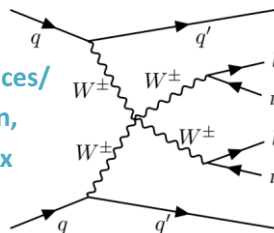
| | Expected [TeV ⁻⁴] | Observed [TeV ⁻⁴] |
|---------------------|-------------------------------|-------------------------------|
| f_{T0}/Λ^4 | [-0.80, 0.80] | [-0.57, 0.56] |
| f_{T1}/Λ^4 | [-0.52, 0.49] | [-0.39, 0.35] |
| f_{T2}/Λ^4 | [-1.6, 1.4] | [-1.2, 1.0] |
| f_{M0}/Λ^4 | [-8.3, 8.3] | [-5.8, 5.6] |
| f_{M1}/Λ^4 | [-12.3, 12.2] | [-8.6, 8.5] |
| f_{M7}/Λ^4 | [-16.2, 16.2] | [-11.3, 11.3] |
| f_{S02}/Λ^4 | [-14.2, 14.2] | [-10.4, 10.4] |
| f_{S1}/Λ^4 | [-42, 41] | [-30, 30] |

- Evaluation of relevant limits as a function of the unitarisation cut-off

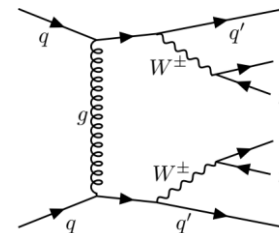


- Largest **EW** to **QCD** production ratio among final states sensitive to **VBS**
- Triboson production with 1 hadronic decay suppressed in EW VBS phase space region ($\rightarrow m_{jj}$)

EW
VBS with triple/quartic vertices/
exchange of a higgs boson,
no s-channel triple vertex
& non-VBS



QCD
w/o gg & gg
initial states



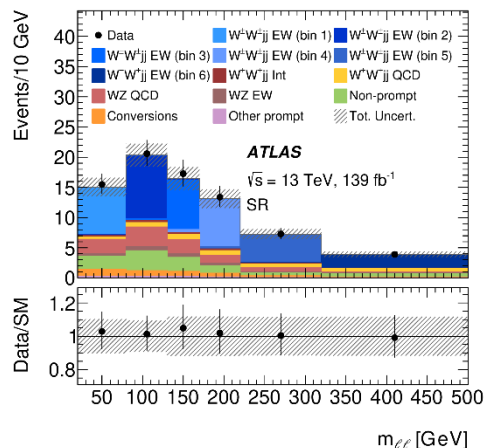
- **Clean signature:** 2 same-charged leptons (e, μ), $\geq 2j$ (high m_{jj} & $|\Delta y_{jj}|$) & E_T^{miss}
- Dominant WZ/γ^* and non-prompt lepton background

EW $W^\pm W^\pm jj$ & inclusive cross-section measurements

- Cross-section from maximum likelihood fits with signal strength of SR & WZ CR (m_{jj} reduced) as free parameter
- **Most precise $W^\pm W^\pm jj$ fiducial measurements to date!**

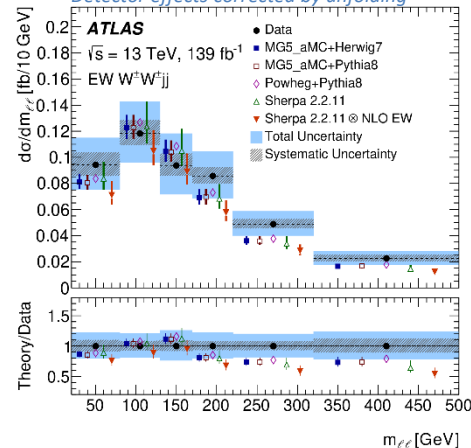
$$\frac{\sigma_{\text{fid}}^{\text{EW}} [\text{fb}]}{2.92 \pm 0.22 (\text{stat.}) \pm 0.19 (\text{syst.})} \quad \frac{\sigma_{\text{fid}}^{\text{EW+Int+QCD}} [\text{fb}]}{3.38 \pm 0.22 (\text{stat.}) \pm 0.19 (\text{syst.})}$$

Very good data/MC agreement!



EW $W^\pm W^\pm jj$

Detector effects corrected by unfolding



aQGC

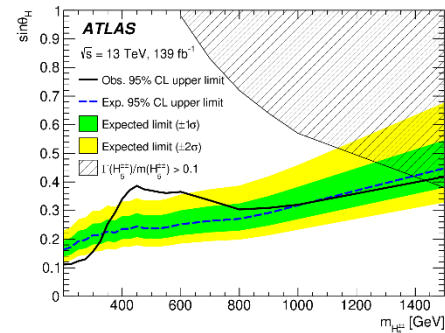
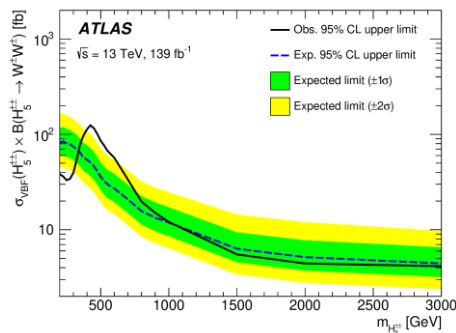
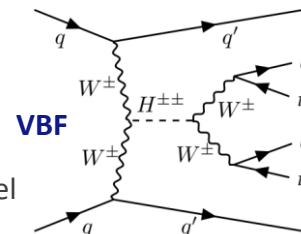
- Limits on 9 relevant D-8 EFT operators at 95% CL from the m_{ll} distribution in both SR & CRs

| Coefficient | Type | No unitarisation cut-off [TeV ⁻⁴] | Lower, upper limit at the respective unitarity bound [TeV ⁻⁴] |
|---------------------|------|---|---|
| f_{M0}/Λ^4 | Exp. | [-3.9, 3.8] | -64 at 0.9 TeV, 40 at 1.0 TeV |
| | Obs. | [-4.1, 4.1] | -140 at 0.7 TeV, 117 at 0.8 TeV |
| f_{M1}/Λ^4 | Exp. | [-6.3, 6.6] | -25.5 at 1.6 TeV, 31 at 1.5 TeV |
| | Obs. | [-6.8, 7.0] | -45 at 1.4 TeV, 54 at 1.3 TeV |
| f_{M7}/Λ^4 | Exp. | [-9.3, 8.8] | -33 at 1.8 TeV, 29.1 at 1.8 TeV |
| | Obs. | [-9.8, 9.5] | -39 at 1.7 TeV, 42 at 1.7 TeV |
| f_{S02}/Λ^4 | Exp. | [-5.5, 5.7] | -94 at 0.8 TeV, 122 at 0.7 TeV |
| | Obs. | [-5.9, 5.9] | - |
| f_{S1}/Λ^4 | Exp. | [-22.0, 22.5] | - |
| | Obs. | [-23.5, 23.6] | - |
| f_{T0}/Λ^4 | Exp. | [-0.34, 0.34] | -3.2 at 1.2 TeV, 4.9 at 1.1 TeV |
| | Obs. | [-0.36, 0.36] | -7.4 at 1.0 TeV, 12.4 at 0.9 TeV |
| f_{T1}/Λ^4 | Exp. | [-0.158, 0.174] | -0.32 at 2.6 TeV, 0.44 at 2.4 TeV |
| | Obs. | [-0.174, 0.186] | -0.38 at 2.5 TeV, 0.49 at 2.4 TeV |
| f_{T2}/Λ^4 | Exp. | [-0.56, 0.70] | -2.60 at 1.7 TeV, 10.3 at 1.2 TeV |
| | Obs. | [-0.63, 0.74] | - |

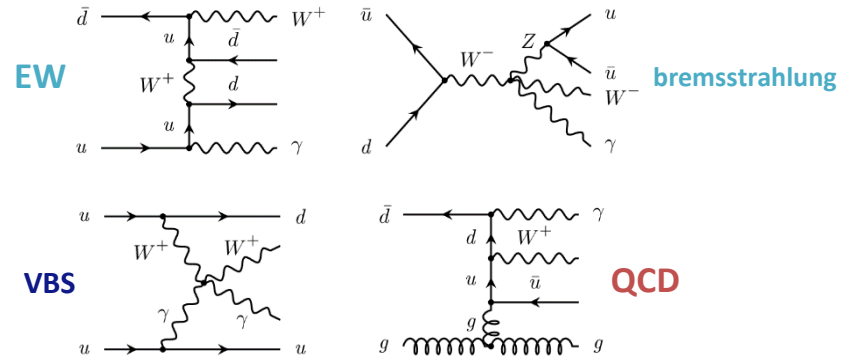
- Evaluation of limits as a function of the unitarisation cut-off excludes zero-values for f_{M0} , f_{S1} , f_{S02} , f_{T0} for clipping scales below ~ 1 TeV at 95% CL
- Additional 2D limits on operator pairs

Search for doubly-charged Higgs boson production

- Evaluation of the m_T distribution in context of the Georgi-Machacek model
- Upper limits on $\sin \Theta_H$ & $\sigma_{\text{VBF}}(H_5^{\pm\pm}) \times B(H_5^{\pm\pm} \rightarrow W^\pm W^\pm)$ at 95% CL
- $\sin \Theta_H > 0.11$ -0.42 excluded for $200 \text{ GeV} < m_{H_5^{\pm\pm}} < 1500 \text{ GeV}$
- Local excess of events for $m_{H_5^{\pm\pm}} = 450 \text{ GeV}$ at 2.5 σ



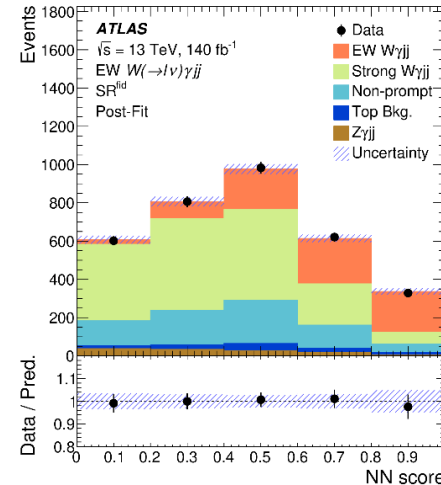
- High precision for differential **EW** W γ jj cross-section measurements compared to other **VBS** processes (large production cross-section)
- Combined measurement of **EW** W γ jj processes in region with enhanced **VBS**
- **Clean signature:** $1e/\mu, p_T^{\text{miss}} \geq 1\gamma, \geq 2j$ (high m_{jj} & $|\Delta y_{jj}|$)
- **QCD** W γ jj dominant prompt background
- Background from misidentified leptons and photons
- Multivariate techniques including a Neural Network to isolate **EW** W γ jj from **QCD** W γ jj
- SR & CRs separated by N_{jets}^{gap} & $\xi_{l\gamma}$



EW W γ jj fiducial cross section measurement

$$\sigma_{EW} = 13.2 \pm 2.5 \text{ fb with } \gg 6\sigma \text{ significance (6.3}\sigma \text{ expected)}$$

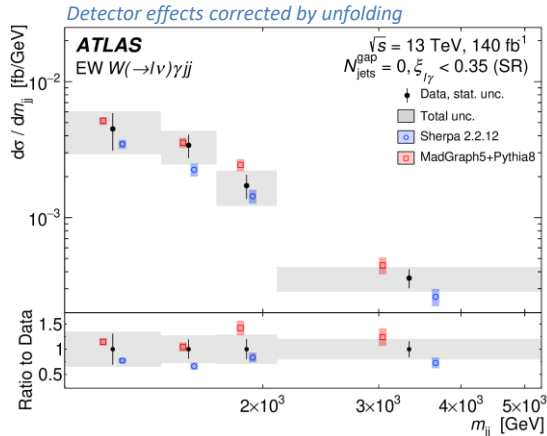
- MADGRAPH5+PYTHIA8 in agreement with data within uncertainties
- $\sim 2\sigma$ underestimation by SHERPA 2.2.12 from the 3rd parton in the SHERPA matrix element



Good data/MC agreement!

EW W_{jj} differential cross section measurements

- Differential measurements for a set of variables sensitive to QGC or the CP violation structure of WWγγ & WWγZ
- Reasonable agreement of data & LO SM prediction
- Slight overestimation of the measurement by MADGRAPH5+PYTHIA8 at high m_{jj} & high p_T^{jj}
- Good shape agreement for SHERPA 2.2.12 but tendency to underestimate



Search for WWγγ & WWγZ (aQGC)

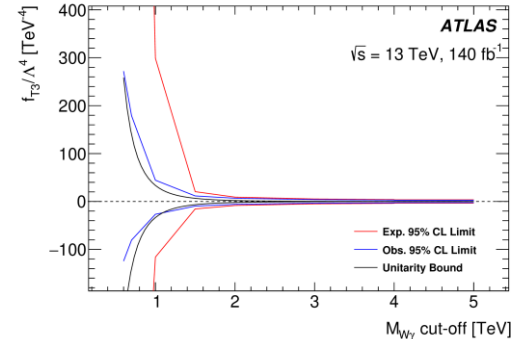
- 95% CL limits on EFT D-8 operators

| Coefficients [TeV ⁻⁴] | Observable | Expected [TeV ⁻⁴] | Observed [TeV ⁻⁴] |
|-----------------------------------|------------------------------|-------------------------------|-------------------------------|
| f _{T0} /Λ ⁴ | p _T ^{jj} | [-2.4, 2.4] | [-1.8, 1.8] |
| f _{T1} /Λ ⁴ | p _T ^{jj} | [-1.5, 1.6] | [-1.1, 1.2] |
| f _{T2} /Λ ⁴ | p _T ^{jj} | [-4.4, 4.7] | [-3.1, 3.5] |
| f _{T3} /Λ ⁴ | p _T ^{jj} | [-3.3, 3.5] | [-2.4, 2.6] |
| f _{T4} /Λ ⁴ | p _T ^{jj} | [-3.0, 3.0] | [-2.2, 2.2] |
| f _{T5} /Λ ⁴ | p _T ^{jj} | [-1.7, 1.7] | [-1.2, 1.3] |
| f _{T6} /Λ ⁴ | p _T ^{jj} | [-1.5, 1.5] | [-1.0, 1.1] |
| f _{T7} /Λ ⁴ | p _T ^{jj} | [-3.8, 3.9] | [-2.7, 2.8] |
| f _{M0} /Λ ⁴ | p _T ^l | [-28, 28] | [-24, 24] |
| f _{M1} /Λ ⁴ | p _T ^l | [-43, 44] | [-37, 38] |
| f _{M2} /Λ ⁴ | p _T ^l | [-10, 10] | [-8.6, 8.5] |
| f _{M3} /Λ ⁴ | p _T ^l | [-16, 16] | [-13, 14] |
| f _{M4} /Λ ⁴ | p _T ^l | [-18, 18] | [-15, 15] |
| f _{M5} /Λ ⁴ | p _T ^l | [-17, 14] | [-14, 12] |
| f _{M7} /Λ ⁴ | p _T ^l | [-78, 77] | [-66, 65] |

Observable most sensitive to tensor-type operators

Observable most sensitive to mixed scalar operators

- Additional constraints with unitarity preservation are obtained by applying the clipping technique
- First LHC constraints on f_{T3} and f_{T4}



- Several exciting results by the 6 ATLAS analyses presented!

ZZ at 13.6 TeV

- Extension of diboson studies to a new centre-of-mass energy
- Good agreement with SM predictions!

ZZ polarisation & CP

- Observation of $Z_L Z_L$ at 4.3σ
- First constraints on CP-odd aNTGC (SM-EFT interference)

WZ polarisation at high p_T

- First time study of RAZ effect in WZ
- Observation of 00 WZ polarisation at 5.2σ in $100 < p_T^Z < 200$ GeV

$W^\pm Zjj$

- Most precise $W^\pm Zjj$ EW cross-section measurement
- Constraints on aQGC

$W^\pm W^\pm jj$

- Constraints on aQGC
- Search for $H^{\pm\pm}$

$W\gamma jj$

- Constraints on aQGC
- First LHC constraints on the f_{T3} & f_{T4} operators of the EFT framework

Backup

ZZ at 13.6 TeV

13.6 TeV 29 fb⁻¹ Partial Run-3



| Source | Relative uncertainty(%) |
|------------------------------|-------------------------|
| Data statistical uncertainty | 4.2 |
| MC statistical uncertainty | 0.3 |
| Luminosity | 2.2 |
| Lepton momentum | 0.2 |
| Lepton efficiency | 3.7 |
| Background | 1.6 |
| Theoretical uncertainty | 1.0 |
| Total | 6.3 |

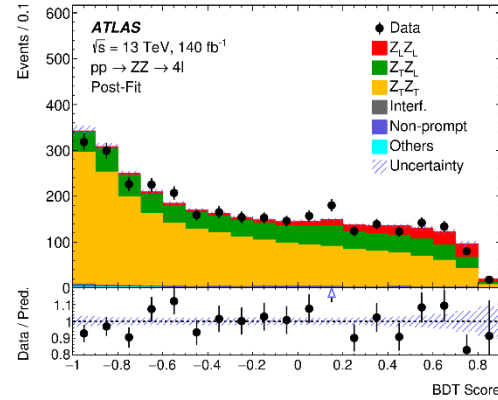
ZZ polarisation & CP

13 TeV 140 fb⁻¹ Full Run-2

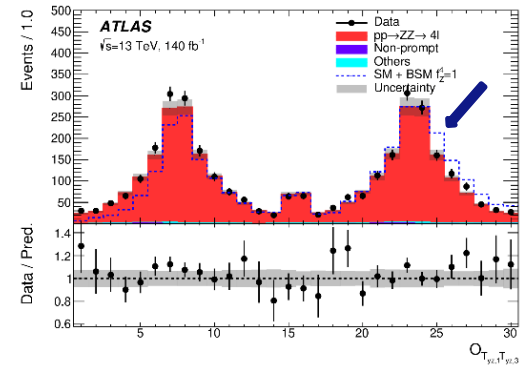


| Contribution | Relative uncertainty [%] |
|---|--------------------------|
| Total | 24 |
| Data statistical uncertainty | 23 |
| Total systematic uncertainty | 8.8 |
| MC statistical uncertainty | 1.7 |
| Theoretical systematic uncertainties | |
| $q\bar{q} \rightarrow ZZ$ interference modelling | 6.9 |
| NLO reweighting observable choice for $q\bar{q} \rightarrow ZZ$ | 3.7 |
| PDF, α_s and parton shower for $q\bar{q} \rightarrow ZZ$ | 2.2 |
| NLO reweighting non-closure | 1.0 |
| QCD scale for $q\bar{q} \rightarrow ZZ$ | 0.2 |
| NLO EW corrections for $q\bar{q} \rightarrow ZZ$ | 0.2 |
| $gg \rightarrow ZZ$ modelling | 1.4 |
| Experimental systematic uncertainties | |
| Luminosity | 0.8 |
| Muons | 0.6 |
| Electrons | 0.4 |
| Non-prompt background | 0.3 |
| Pile-up reweighting | 0.3 |
| Triboson and $t\bar{t}Z$ normalisations | 0.1 |

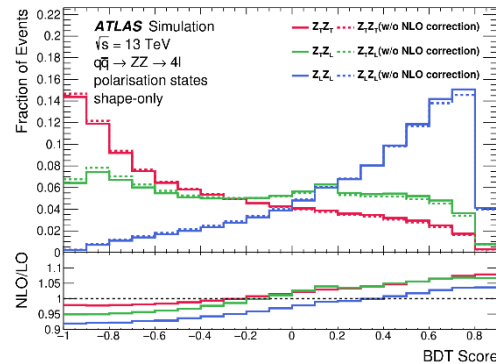
BDT distribution



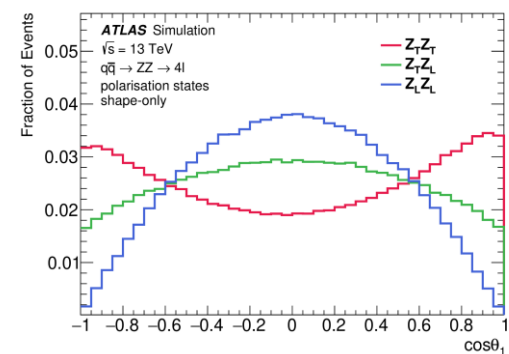
Asymmetric prediction



Impact of NLO corrections



Detector-level distribution to train BDT



(RAZ) effect in WZ

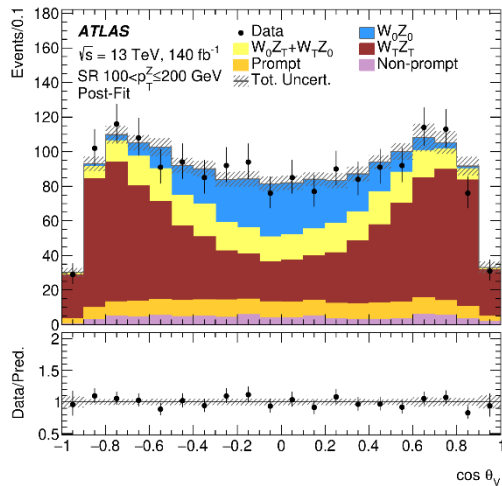
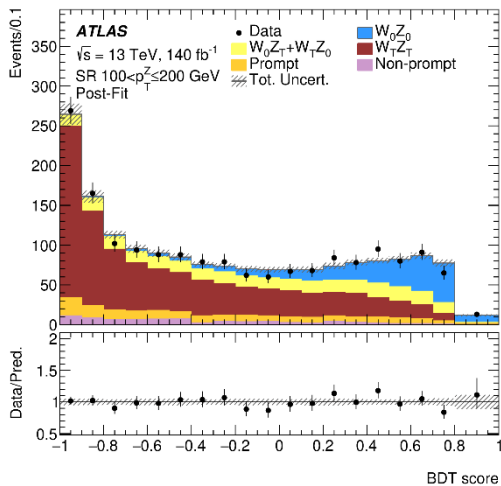
| Source | Impact [%] | | | |
|--|----------------------|----------------|----------------------|----------------|
| | TT state | | Sum of polarizations | |
| $p_T^{WZ} < 70 \text{ GeV}$ | $\Delta Y(\ell_W Z)$ | $\Delta Y(WZ)$ | $\Delta Y(\ell_W Z)$ | $\Delta Y(WZ)$ |
| Experimental | | | | |
| Luminosity | 1.5 | 0.6 | 0.5 | 0.1 |
| Electron calibration | 0.9 | 0.5 | 1.7 | 0.4 |
| Muon calibration | 1.6 | 0.8 | 1.4 | 0.5 |
| Jet energy scale and resolution | 3.4 | 1.9 | 1.8 | 1.2 |
| E_T^{miss} scale and resolution | 1.3 | 1.0 | 2.2 | 1.4 |
| Flavor-tagging inefficiency | 0.0 | 0.0 | 0.1 | 0.0 |
| Pileup modelling | 0.0 | 0.4 | 3.4 | 0.4 |
| Non-prompt background estimation | 9.5 | 3.6 | 13.5 | 3.7 |
| Modelling | | | | |
| Background, other | 5.7 | 2.1 | 8.0 | 2.1 |
| Model statistical | 2.4 | 1.3 | 4.6 | 2.0 |
| NLO corrections | 9.2 | 1.0 | 0.0 | 0.0 |
| PDF, Scale and shower settings | 7.5 | 3.9 | 0.7 | 0.2 |
| Unfolding uncertainty | 0.0 | 2.3 | 0.0 | 2.6 |
| Experimental and modelling | 17.0 | 6.8 | 17.2 | 5.7 |
| Data statistical | 12.8 | 6.2 | 27.0 | 10.3 |
| Total | 21.3 | 9.3 | 32.0 | 11.8 |

Energy dependence of diboson polarisation fractions

| Source | Impact on f_{00} [%] | |
|---|------------------------------------|---------------------------|
| | $100 < p_T^Z \leq 200 \text{ GeV}$ | $p_T^Z > 200 \text{ GeV}$ |
| Experimental | | |
| Luminosity | 0.1 | 0.2 |
| Electron calibration | 1.0 | 0.9 |
| Muon calibration | 1.1 | 1.3 |
| Jet energy scale and resolution | 5.9 | 9.0 |
| E_T^{miss} scale and resolution | 1.0 | 0.6 |
| Flavor-tagging inefficiency | 0.1 | 0.2 |
| Pileup modelling | 1.6 | 1.1 |
| Non-prompt background estimation | 5.8 | 0.8 |
| Modelling | | |
| Background, other | 1.4 | 1.6 |
| Model statistical | 2.5 | 5.6 |
| NLO QCD effects | 6.8 | 8.2 |
| NLO EW effects | 1.1 | 3.3 |
| Effect of additive vs multiplicative QCD+EW combination | 1.3 | 3.8 |
| Interference impact | 1.4 | 0.7 |
| PDF, Scales, and shower settings | 3.5 | 9.2 |
| Experimental and modelling | 12.1 | 17.7 |
| Data statistical | 18.0 | 64.5 |
| Total | 21.7 | 66.9 |

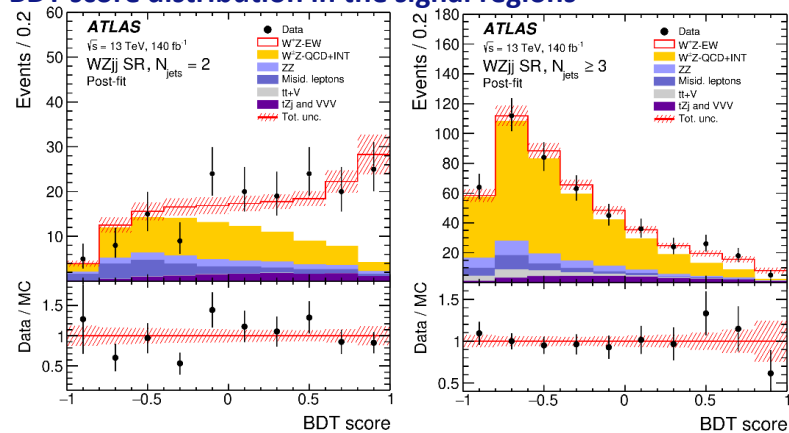
WZ polarisation at high p_T

13 TeV 140 fb⁻¹ Full Run-2

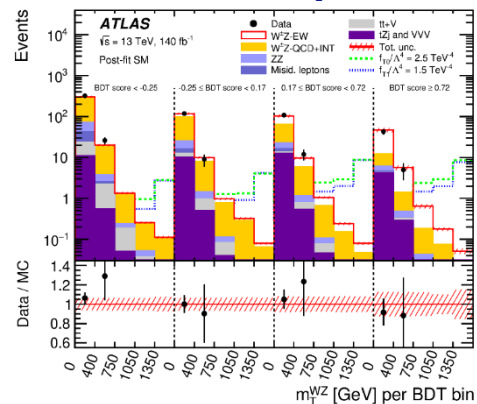


| Source | $\frac{\Delta\sigma_{WZjj-EW}}{\sigma_{WZjj-EW}}$ [%] | $\frac{\Delta\sigma_{WZjj-strong}}{\sigma_{WZjj-strong}}$ [%] |
|--|---|---|
| $WZjj$ -EW theory modelling | 7 | 1.8 |
| $WZjj$ -QCD theory modelling | 2.8 | 8 |
| $WZjj$ -EW and $WZjj$ -QCD interference PDFs | 0.35 | 0.6 |
| Jets | 2.3 | 5 |
| Pile-up | 1.1 | 0.6 |
| Electrons | 0.8 | 0.8 |
| Muons | 0.9 | 0.9 |
| b -tagging | 0.10 | 0.11 |
| MC statistics | 1.9 | 1.2 |
| Misid. lepton background | 2.3 | 2.3 |
| Other backgrounds | 0.9 | 0.23 |
| Luminosity | 0.7 | 0.9 |
| All systematics | 16 | 12 |
| Statistics | 10 | 6 |
| Total | 19 | 13 |

BDT score distribution in the signal regions



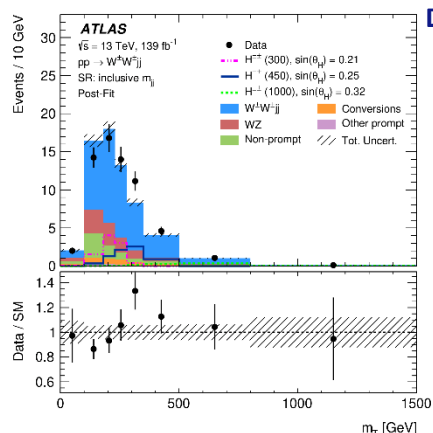
2D combination of BDT score and m_T^{WZ} to obtain the EFT limits



$W^\pm W^\pm jj$

13 TeV 139 fb⁻¹ Full Run-2

| Source | Impact [%] |
|--|------------|
| Experimental | 4.6 |
| Electron calibration | 0.4 |
| Muon calibration | 0.5 |
| Jet energy scale and resolution | 1.9 |
| E_T^{miss} scale and resolution | 0.2 |
| b -tagging inefficiency | 0.7 |
| Background, misid. leptons | 3.4 |
| Background, charge misrec. | 1.0 |
| Pile-up modelling | 0.1 |
| Luminosity | 1.9 |
| Modelling | 4.5 |
| EW $W^\pm W^\pm jj$, shower, scale, PDF & α_s | 0.7 |
| EW $W^\pm W^\pm jj$, QCD corrections | 1.9 |
| EW $W^\pm W^\pm jj$, EW corrections | 0.9 |
| Int $W^\pm W^\pm jj$, shower, scale, PDF & α_s | 0.6 |
| QCD $W^\pm W^\pm jj$, shower, scale, PDF & α_s | 2.6 |
| QCD $W^\pm W^\pm jj$, QCD corrections | 0.8 |
| Background, WZ scale, PDF & α_s | 0.3 |
| Background, WZ reweighting | 1.5 |
| Background, other | 1.3 |
| Model statistical | 1.8 |
| Experimental and modelling | 6.4 |
| Data statistical | 7.4 |
| Total | 9.8 |



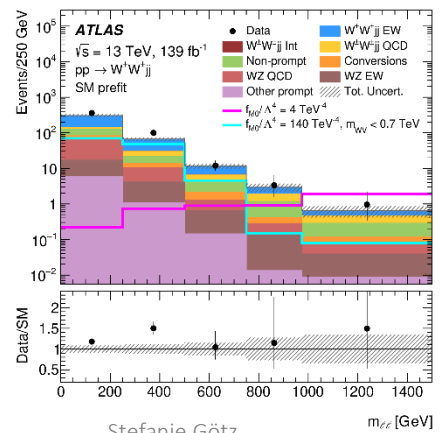
Distribution for $H_{5^{\pm\pm}}$ search

JHEP 04 (2024) 026, STDM-2018-32

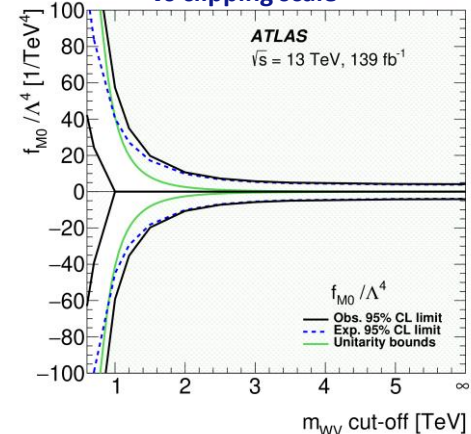
- The differential measurements are for all parameters except m_T well described

| Variable | EW $W^\pm W^\pm jj$ | | Inclusive $W^\pm W^\pm jj$ | | Max. value in data |
|-----------------------|-------------------------|------------|----------------------------|------------|--------------------|
| | χ^2/N_{dof} | p -value | χ^2/N_{dof} | p -value | |
| $m_{\ell\ell}$ | 4.5/6 | 0.605 | 7.34/6 | 0.291 | 1081 GeV |
| m_T | 13.0/6 | 0.043 | 16.33/6 | 0.012 | 1270 GeV |
| m_{jj} | 7.6/6 | 0.266 | 8.67/6 | 0.193 | 6328 GeV |
| $N_{\text{gap jets}}$ | 2.5/2 | 0.282 | 2.53/2 | 0.282 | 5 |
| ξ_{J3} | 4.2/5 | 0.517 | 4.93/5 | 0.424 | 1.74 |

Distribution for aQGC limits

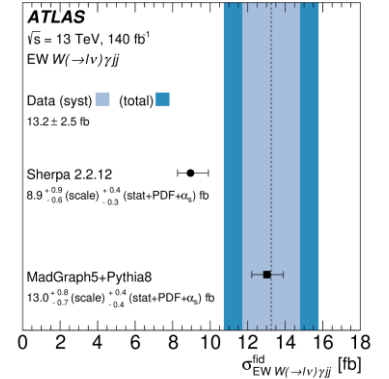


Example of 1D limit on D-8 EFT operators vs clipping scale

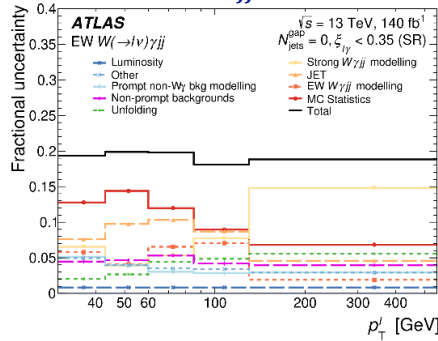
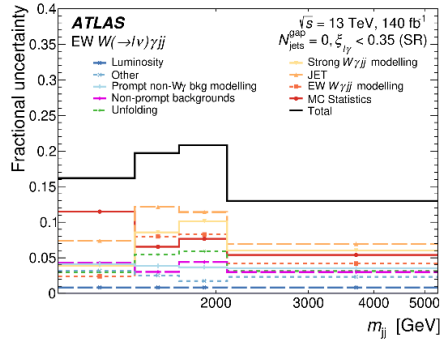


| Uncertainty Source | Fractional Uncertainty [%] |
|-------------------------------|----------------------------|
| MC Statistics | 11 |
| Jets | 8 |
| Lepton, photon, pile-up | 8 |
| EW $W\gamma jj$ modelling | 7 |
| Data Statistics | 6 |
| Strong $W\gamma jj$ modelling | 6 |
| Non-prompt background | 2 |
| Luminosity | 2 |
| Other Background modelling | 2 |
| E_T^{miss} | 1 |

| Fiducial cross-section | SR ^{fid} | | CR ^{fid} | |
|----------------------------|--|--|--|--|
| | $N_{\text{jets}}^{\text{gap}} = 0$ | | $N_{\text{jets}}^{\text{gap}} > 0$ | |
| Differential cross-section | SR | CR _A | CR _B | CR _C |
| $m_{jj} > 1 \text{ TeV}$ | $N_{\text{jets}}^{\text{gap}} = 0$ $\xi_{l\gamma} < 0.35$ | $N_{\text{jets}}^{\text{gap}} > 0$ $\xi_{l\gamma} < 0.35$ | $N_{\text{jets}}^{\text{gap}} > 0$ $0.35 < \xi_{l\gamma} < 1$ | $N_{\text{jets}}^{\text{gap}} = 0$ $0.35 < \xi_{l\gamma} < 1$ |



Fractional uncertainties as a function of m_{jj} & p_T^l



Distribution for predicted and observed yields as a function of m_{jj}

